Journal of Magnetic Resonance 196 (2009) 101–104

Contents lists available at ScienceDirect

Journal of Magnetic Resonance

journal homepage: www.elsevier.com/locate/jmr

# Low-field NMR measurement procedure when SQUID detection is used

Longqing Qiu [a,b,*], Yi Zhang [a], Hans-Joachim Krause [a], Alex I. Braginski [a], Andreas Offenhäusser [a]

[a] Institute of Bio- and Nanosystems, Research Center Juelich, D-52425 Juelich, Germany
[b] Pohl Institute of Solid State Physics, Tongji University, Shanghai 200092, PR China

ARTICLE INFO

*Article history:*
Received 9 June 2008
Revised 8 September 2008
Available online 17 September 2008

*Keywords:*
NMR
SQUID
Low field
Pre-polarization
Adiabatical
Nonadiabatical

ABSTRACT

In reported low-field nuclear magnetic resonance (NMR) measurements using Superconducting Quantum Interference Device (SQUID) detection, the pre-polarizing magnetic field has been usually oriented orthogonal to the measuring field, $B_p \perp B_m$. Melton et al. systematically analyzed the consequences of $B_p$ decay in time after turnoff and showed that this decay should be nonadiabatic. We evaluated our measuring procedure in the light of that analysis, and found good quantitative agreement. It was showed that, when the decay time constant is comparable to the precession period of the magnetization of the sample, $\boldsymbol{M}$, the optimum procedure is to orient $B_p$ parallel to $B_m$ and to apply a $\pi/2$ pulse to flip $\boldsymbol{M}$, similar as in the case of conventional NMR.



## 1. Introduction

In nuclear magnetic resonance (NMR) spectroscopy and magnetic resonance imaging (MRI), the general trend has been to higher measurement fields in order to improve the signal intensity and resolution. In conventional NMR systems, there is only one high magnetic field $B$ in the tesla (T) range, which acts both as the polarizing and measuring field. To detect the precession of $\boldsymbol{M}$ as function of time, and the resulting free induction decay (FID) signal, one usually applies a radio frequency (rf) pulse near the Larmor frequency $f_L$. This pulse, applied perpendicular to $B$, deviates the magnetization vector $\boldsymbol{M}$ of the sample from the start position. The rf pulse is called the $\pi/2$ pulse when it is applied to deviate $\boldsymbol{M}$ nearly perpendicular to its start position.[1]

Recently, a renewed interest in low-field NMR measurements has been motivated by the use of Superconducting Quantum Interference Devices (SQUIDs) as sensitive and frequency-independent magnetic flux detectors [1,2]. The measurement arrangement in low-field NMR is quite different than at high fields. Usually, two independent magnetic fields, the stronger pre-polarizing field ($B_p$) and the weak measurement field ($B_m$), are applied, with $B_p \perp B_m$. It is assumed that the magnetization $\boldsymbol{M}$ of the sample after turning off $B_p$ is still nearly perpendicular to $B_m$. Such low-field NMR measurements are discussed, for example, in [2–6].

The innate limitation of low-field NMR is its low signal-to-noise ratio (SNR). To partially overcome this limitation, an effective and simple method is to increase $B_p$, as $|\boldsymbol{M}|$ is proportional to $B_p$. When $B_p$ is generated by coils, a larger inductance, $L_{Bp}$, and/or higher current are needed to generate higher $B_p$. After $B_p$ is turned off, the $B_p$ decay time constant $\tau = L_{Bp}/R$, where $R$ is the discharge resistor, will determine the initial position of $\boldsymbol{M}$. The need to introduce an ac pulse occurs when $\tau$ is comparable to the $\boldsymbol{M}$ precession period (the $f_L$ at low $B_m$ is below the radio frequency range, hence we write ac instead of rf). For example, McDermott et al. increased $B_p$ up to 300 mT, and introduced a $\pi/2$–$\pi$ ac pulse sequence after turning off of $B_p$ to detect the spin-echo signal [7]. Similarly, Yang et al. applied a $\pi/2$ pulse after $B_p$ to record the FID signal [8].

Naturally, the use and orientation of $B_p$, the effects of magnetic field inhomogeneity, the relation between $\tau$ and $\boldsymbol{M}$ precession period, and the application of ac pulse(s) were already considered in early work on Earth's field NMR and on low-cost MRI using a Faraday coil detector [9–12]. Melton et al. systematically investigated the $B_p$ decay process by solving the equation of motion $d\boldsymbol{M}/dt = \gamma \boldsymbol{M} \times \boldsymbol{B}$, where $\gamma$ is the gyromagnetic ratio (proton gyromagnetic ratio equals $2.68 \times 10^8$ rad/Ts), and analyzing the regimes of "sudden passage" ($B_p$ is reduced quickly and $\boldsymbol{M}$ left behind to precess about $B_m$) and "adiabatic passage" ($B_p$ is reduced so slowly that $\boldsymbol{M}$ follows it and aligns with $B_m$ without any precession occurring) [13,14].

The purpose of our present paper is to experimentally evaluate the low-field measuring procedures in the light of Melton et al. analysis while using a SQUID detector. Our results suggest that the optimum procedure, when $\tau$ is comparable to the $\boldsymbol{M}$ precession period, is to apply $B_p$ parallel to $B_m$ ($B_p \parallel B_m$) and to apply a $\pi/2$ ac pulse to flip $\boldsymbol{M}$, similar as in the case of conventional NMR.

* Corresponding author. Address: Institute of Bio- and Nanosystems, Research Center Juelich, D-52425 Juelich, Germany. Fax: +49 2461 612630.
*E-mail address:* l.qiu@fz-juelich.de (L. Qiu).

[1] For rapid NMR imaging angles much lower than $\pi/2$ are also used.

1090-7807/$ - see front matter © 2008 Elsevier Inc. All rights reserved.
doi:10.1016/j.jmr.2008.09.009

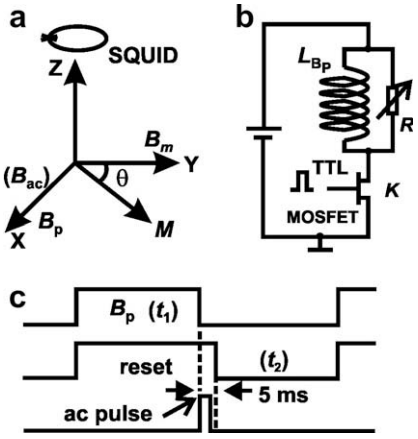


**Fig. 1.** Measurement details. (a) Orientations of measurement field $B_m$, polarization field $B_p$, ac pulse field $B_{ac}$, and the sensitive direction of the SQUID. ***M*** indicates the orientation of the magnetization after $B_p$ decayed to zero, and $\theta$ is the cone angle between ***M*** and $B_m$. (b) The pre-polarization field circuit: a variable resistor R shunts the coil in order to change the decay time of the polarization field $B_p$; the circuit is switched by a MOSFET controlled by TTL sequence. (c) Pulse sequence for $B_p$, $B_{ac}$ and SQUID readout electronics. The 1 ms delay between the $B_p$ turnoff and $B_{ac}$ application is not shown in the diagram. The electronics is kept in the reset state during the high level of the TTL pulse.

## 2. Measurement methods

We performed low-field NMR measurements inside a magnetically shielded room (MSR) using a high-$T_c$ SQUID as the signal detector.[2] The correlations between the $B_p$ decay time constant $\tau$, ***M*** precession period, and its amplitude were investigated quantitatively. The signal outputs were compared with those simulated in [14]. We then compared FID and spin echo signals recorded by using two arrangements, $B_p \perp B_m$ and $B_p \parallel B_m$.

The nitrogen-cooled rf SQUID magnetometer was positioned inside a fiberglass cryostat. This magnetometer is a so-called substrate resonator rf SQUID [15]. In MSR, this SQUID exhibits a field resolution of 40 fT $Hz^{-1/2}$ down to tens of Hz. The sample of 10 ml tap water was placed beneath the bottom of the cryostat finger and at the center of a Helmholtz coil pair (radius: $r = 23$ cm). This coil current, $I_m$, generated a homogeneous magnetic field $B_m$ in the sample ($B/I = 0.46$ mT/A). The distance between the sample center and the SQUID was about 25 mm. A 5-layer solenoid (inner diameter 32 mm, length 64 mm, wire diameter 0.4 mm, inductance $L_{Bp} = 7.2$ mH, resistance = 11 Ω) surrounded the sample and was used to generate a pulsed polarization field $B_p$ ($B/I = 10$ mT/A). Its direction was either perpendicular or parallel to $B_m$, but it was always orthogonal to the sensitive direction of the SQUID ($z$-axis). The single-layer ac pulse coil was wound on the outside surface of the polarization coil using the same wire diameter. In the measurement configuration of Fig. 1(a), only $B_p \perp B_m$ is shown for clarity.

To investigate the influence of the $B_p$ decay on the FID signal, the decay time constant $\tau$ was adjusted by varying the discharge resistance $R$ connected across the $B_p$ solenoid as shown in Fig. 1(b). The value of $R$ was varied from 16.5 Ω to 5 kΩ (5 kΩ was the solenoid's permanent protection resistance), corresponding to $\tau$ from 436 to 1.44 μs. The electric switch $K$ was realized by a MOSFET (BUZ 80A) controlled by TTL pulse sequence. The $B_p$ decay time constant $\tau$ was determined from the time dependence of voltage measured across a small resistance (0.2 Ω) in series with the polarization solenoid. The decay constant was defined as the time in which the voltage dropped by 63% ($e^{-1}$) of its maximum initial value. In the case of $B_p = 10$ mT (current: 1 A), the experimentally measured $\tau$ agreed well with the calculated values $L/R$.

Typically, each measurement started by polarizing the sample in $B_p \approx 10$ mT for $t_1 = 10$ s controlled by the switch $K$. After $B_p$ decayed to zero, the sample was left in $B_m$, which was always kept on. The reset time of SQUID readout electronics was preprogrammed to be 5 ms longer than the polarization time $t_1$, and the data acquisition $t_2$ began when the SQUID was put into measurement mode, as shown in Fig. 1(c). Optionally, an ac pulse could be inserted during the 5 ms time interval to recover the loss of signal. The ac pulse was applied 1 ms after the switch-off of $B_p$; its duration was typically between 1 and 3 ms (at longer durations the reset time was extended accordingly). All measurements in our experiments followed this pulse sequence.

To obtain the FID signal, a homemade mixer was used to transfer the signal to lower frequency, The NMR signals were recorded by a Dynamic Signal Analyzer (HP 3562) while using a band filter with a bandwidth of about 10 Hz.

The original intention of orienting $B_p$ perpendicular to $B_m$ has been to simplify the measurement field sequence, and to detect the signal directly after the $B_p$ turnoff. However, the magnetization ***M*** remains in $B_p$ direction only when $B_p$ decays nonadiabatically (sudden passage), i.e., satisfies the following condition [14]:

$$dB_p/dt \gg \gamma B_m^2. \quad (1)$$

This requirement is easily met for a laboratory SQUID instrumentation operating in ultralow field NMR [4]. However, with $B_m$ or $\tau$ increasing, it is increasingly difficult to guarantee the sudden passage condition.

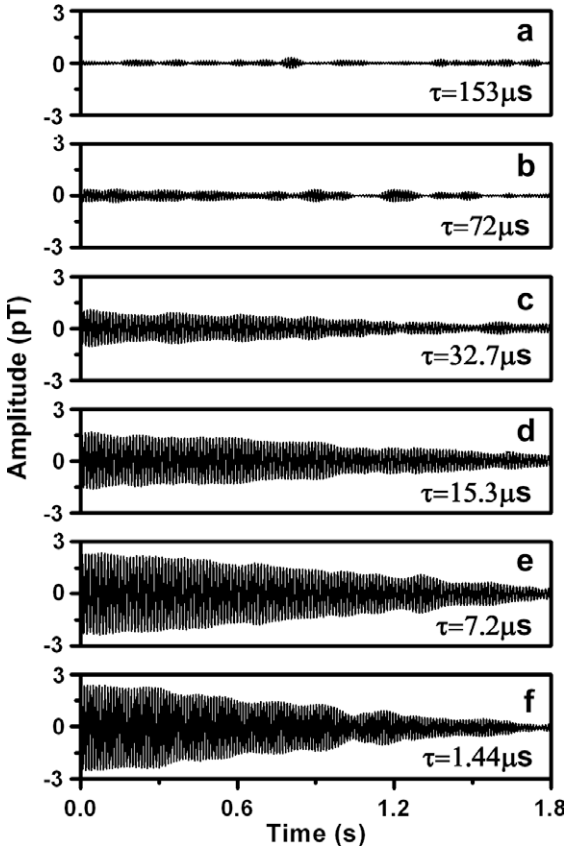


**Fig. 2.** FID signals of 10 ml tap water at $f_L = 4.23$ kHz and values of $\tau$ decreasing from top to bottom (signals averaged, $N = 10$).

[2] There is no merit in using high-$T_c$ SQUID in this work. Simply, this device was available, as we have been interested in mobile applications of low-field NMR.

## 3. Results and discussion

Fig. 2 compares FID traces obtained with different $\tau$, adjusted by varying the discharge resistance $R$. The Larmor frequency of these FID traces is 4.23 kHz ($B_m$ = 99.3 μT), corresponding to the precession period $T_L$ = 236 μs.

In Fig. 2, traces (e) and (f) have almost the same amplitude, which means the sudden passage condition is satisfied. As $\tau$ increases, the FID signal amplitude decreases gradually, and practically disappears in noise when $\tau$ = 153 μs (see the top trace). Note that after $B_p$ circuit is turned off, the sample is left in two fields: the constant $B_m$ and the exponentially decaying $B_p$:

$$B_p = B_{p0}\exp(-t/\tau). \quad (2)$$

The decrease of the original amplitude reflects the orientation of the magnetization $\boldsymbol{M}$ at the beginning of each measurement. Only the component $\boldsymbol{M}\sin\theta$ contributes to the signal, with the precession cone angle $\theta$ between $\boldsymbol{M}$ and $B_m$ decreasing as $\tau$ increases.

In the case that $\tau$ is two orders of magnitude shorter than $T_L$, $B_p$ decays nonadiabatically. After $B_p$ decayed off, $\boldsymbol{M}$ still lags behind, and is almost on the $x$-axis of Fig. 1(a). We thus detect the full signal, as in Fig. 2(e) and (f). As $\tau$ increases, $\boldsymbol{M}$ follows the resulting field $B$ more and more closely and ends up precessing around $B_m$ in a small cone angle $\theta$. According to [14], the relationship between $\theta$ and $B_m$ can be expressed as follows:

$$\theta = \begin{cases} 2\,e^{-(\pi/2)\Gamma}, & (\Gamma \geqslant 1), \\ (1-\Gamma)\cdot\pi/2, & (\Gamma \leqslant 0.4). \end{cases} \quad (3)$$

Here, $\Gamma = \omega_m\tau$ is defined as a dimensionless measure of the decay time constant.

Fig. 3 compares the experimental results from Fig. 2 with theoretical values obtained using $\theta$ from Eq. (3). They fit rather well, within an allowable error.

We investigated also FID signals obtained by varying $\tau$ at $f_L$ = 1.5 kHz ($T_L$ = 667 μs) and 10 kHz ($T_L$ = 100 μs). At 1.5 kHz, the signal disappeared when $\tau$ = 436 μs, while at 10 kHz no NMR measurable signal remained when $\tau$ = 32 μs. These results also agree well with Eq. (3).

In the case of $\theta \neq 90°$, the magnetization vector $\boldsymbol{M}$ has a component in $y$-axis, but it can be rotated back to orthogonal position by a $\pi/2$ pulse in $x$-direction, as shown in Fig. 1(a). Fig. 4 shows the signal recovery by an ac pulse when $B_p \perp B_m$. After $B_p$ was switched off, we applied a short $B_{ac}$ pulse aligned with $B_p$, as also indicated in Fig. 1(a). The amplitude of this ac pulse was 4 μT, its frequency was close to $f_L$ = 4.23 kHz, and its duration varied from 236 μs to 6 ms (the number of periods varied from 1 to 26). When the ac pulse

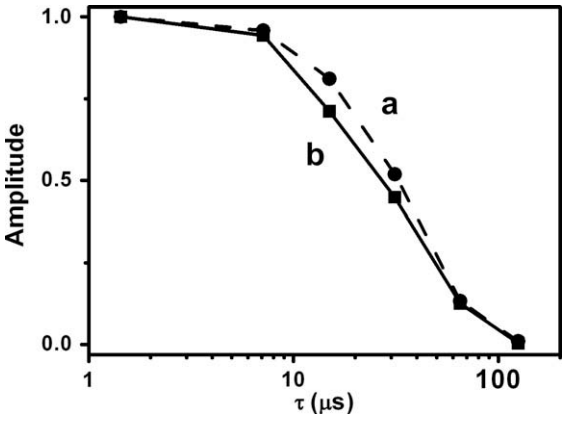


**Fig. 3.** Theoretical (a) and experimental (b) normalized initial amplitude of FID signals versus $\tau$; $f_L$ = 4.23 kHz ($T_L$ = 236 μs).

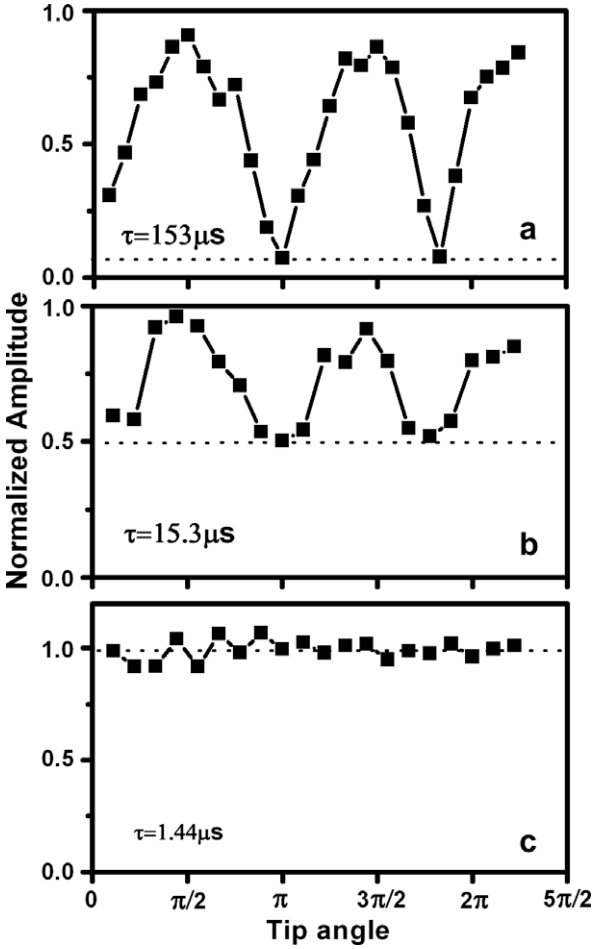


**Fig. 4.** The normalized amplitude versus the tip angle in three typical cases when $f_L$ = 4.23 kHz, $B_p \perp B_m$. When the tip angle > 3π/2 (the ac pulse time lasted > 4 ms), the reset time of SQUID readout electronics was extended correspondingly. The dotted line in each panel shows the signal level without the ac pulse.

lasted 1.3 ms, the condition of orthogonality ($\pi/2$) was fulfilled. We plotted the signal amplitude versus the tip angle for three different $\tau$ values.

As shown in Fig. 4(a), when $\tau$ was long and the residual $\theta$ small, the precessing signal in the $x$–$z$-plane was so small that it became submerged by the noise of our SQUID system. However, the ac pulse recovered the signal back to the value of Fig. 2(f) at tip angle values of $\pi/2, 3\pi/2, 5\pi/2, \ldots$. In the case of Fig. 4(b), $\tau$ was shorter, and the signal was already measurable without the ac-pulse. It represented about 0.5 of the full value, but the ac pulse of appropriated length recalled it fully back. Curve (c), corresponding to a sufficiently short $\tau$, illustrates that no ac-pulse was needed, as in the case of Fig. 2(e) and (f). Here, $B_p$ decayed quickly enough (nonadiabatically), and $\boldsymbol{M}$ was still near the $x$-axis ($\theta = \pi/2$) after $B_p$ already decayed.

The results of Fig. 4 show (when $B_p \perp B_m$), that the progressing decay of $B_p$ causes the initial orientation of $\boldsymbol{M}$ to increasingly deviate from $\theta = \pi/2$, thus adversely affecting the NMR signal. In the case of adiabatical decay ($\Gamma \gg 1$), when $B_p$ decayed to zero the direction of $\boldsymbol{M}$ was already approaching that of $B_m$. In this case, the $\pi/2$ pulse was mandatory to obtain the NMR signal. This observation encouraged us to compare these results with those of the conventional high-field NMR field configuration, which we obtained by reorienting the pre-polarization coil to align $B_p$ with $B_m$.

Fig. 5 compares the averaged ($N$ = 50) FID and spin-echo signals for the two cases, $B_p \perp B_m$ and $B_p \parallel B_m$, at $B_m$ = 99.3 μT

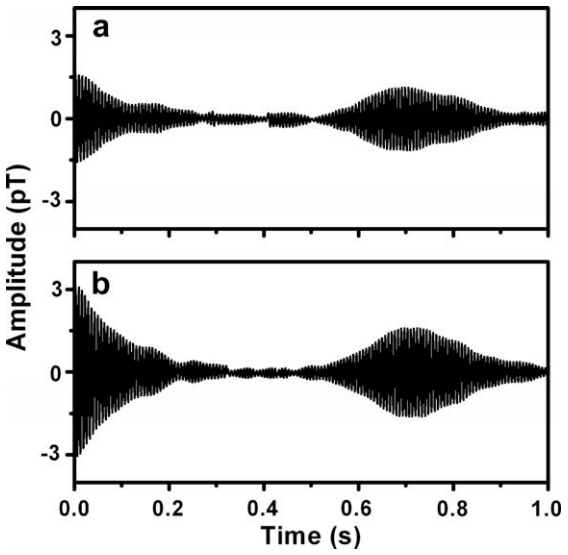


**Fig. 5.** FID and a spin-echo signal when (a) $B_p \perp B_m$ and (b) $B_p \parallel B_m$. The $\pi$ pulse was applied at 350 ms after the switch-off of $B_p$ and lasted 2.6 ms. In both cases, $\tau$ = 153 μs, $f_L$ = 4.32 kHz, with signal averaged ($N$ = 50).

($f_L$ = 4.23 kHz) and the $\tau$ of 153 μs (adiabatic decay). An about 30% stronger signal can be detected when $B_p \parallel B_m$. This is because in this configuration the resulting vector field $\boldsymbol{B}$ would not change its orientation, but only the amplitude. The generated $\boldsymbol{M}$ remains in $B_p$ direction nearly perfectly until flipped by the $\pi/2$ ac pulse. Therefore, $B_p \parallel B_m$ helps avoiding any signal loss due to the imperfect fulfilment of the nonadiabatic switching criterion. Further comparisons were also performed at two other $\tau$ values of 15.3 and 1.44 μs, and results similar to those of Fig. 5 were obtained. The pre-programmed 5 ms delay time is much longer than $5\tau$. Therefore, when $B_p \parallel B_m$, the falling edge of $B_p$ does not affect the stability of $B_m$ during the signal acquisition. We note that the duration of $\pi/2$ and $\pi$ pulse is two orders of magnitude shorter than the measured relaxation time, so the relaxation of the spin population during the application of ac pulses can be safely ignored.

## 4. Conclusion

We measured low-field NMR signals of pre-polarized liquid proton sample and investigated experimentally the transition from nonadiabatic to adiabatic decay of $B_p$, i.e., the effect of $B_p$ decay time constant at Larmor frequencies of 1.5, 4.23 and 10 kHz. Our results conformed to the model of Melton et al. [13,14]. In cases close to adiabatic decay, a proper $\pi/2$ ac pulse can largely recover the signal. In such cases, an improved low-field configuration is to align $B_p$ with $B_m$, as in the conventional high-field NMR configuration. This configuration opens the possibility to use a single coil for generating $B_m$ and $B_p$. Our results could assist other researchers currently investigating low-field NMR using a SQUID detector.

## Acknowledgments

The authors thank Dr. Bernhard Bluemich of RWTH Aachen, Germany, Dr. Saburo Tanaka in Toyohashi University of Technology, Japan, and Ms. Hui Dong for helpful discussions.

## References

[1] Ya. Greenberg, Application of superconducting quantum interference devices to nuclear magnetic resonance, Rev. Mod. Phys. 70 (1998) 175–222.
[2] R. McDermott, A.H. Trabesinger, M. Mueck, E.L. Hahn, A. Pines, J. Clarke, Liquid-state NMR and scalar couplings in microtesla magnetic fields, Science 295 (22) (2002) 2247–2249.
[3] A.N. Matlachov, P.L. Volegov, Michelle A. Espy, J.S. George, R.H. Kraus Jr., SQUID detected NMR in microtesla magnetic fields, J. Magn. Reson. 170 (2004) 1–7.
[4] M. Burghoff, S. Hartwig, L. Trahms, J. Bernarding, Nuclear magnetic resonance in the nanotesla range, Appl. Phys. Lett. 87 (2005) 054103.
[5] Y. Zhang, L.Q. Qiu, H.-J. Krause, S. Hartwig, M. Burghoff, L. Trahms, Liquid state nuclear magnetic resonance at low fields using a nitrogen cooled superconducting quantum interference device, Appl. Phys. Lett. 90 (2007) 182503.
[6] L.Q. Qiu, Y. Zhang, H.-J. Krause, A.I. Braginski, M. Burghoff, L. Trahms, Nuclear magnetic resonance in the Earth's magnetic field using a nitrogen-cooled superconducting quantum interference device, Appl. Phys. Lett. 91 (2007) 072505.
[7] R. McDermott, S.K. Lee, B. Haken, A.H. Trabesinger, A. Pines, J. Clarke, Microtesla MRI with a superconducting quantum interference device, PNAS 101 (21) (2004) 7857–7861.
[8] H.C. Yang, S.H. Liao, H.E. Horng, S.L. Kuo, H.H. Chen, S.Y. Yang, Enhancement of nuclear magnetic resonance in microtesla magnetic field with prepolarization field detected with high-$T_c$ superconducting quantum interference device, Appl. Phys. Lett. 88 (2006) 252505.
[9] M.E. Packard, R. Varian, Free nuclear induction in the Earth's magnetic field, Phys. Rev. 93 (1954) 941.
[10] G.J. Béné, Nuclear magnetism of liquid systems in the Earth field range, Phys. Rep. 58 (1980) 213–267.
[11] A. Macovski, S. Conolly, Novel approaches to low-cost MRI, Magn. Reson. Med. 30 (1993) 221–230.
[12] P.T. Callaghan, M. Legros, Nuclear spins in the Earth's magnetic field, Am. J. Phys. 50 (1982) 709–713.
[13] B.F. Melton, V.L. Pollak, T.W. Mayes, B.L. Willis, Condition for sudden passage in the Earth's-field NMR Technique, J. Magn. Reson. A 117 (1995) 164–170.
[14] B.F. Melton, V.L. Pollak, Condition for adiabatic passage in the Earth's-field NMR technique, J. Magn. Reson. 158 (2002) 15–22.
[15] Y. Zhang, J. Schubert, N. Wolters, Substrate resonator for HTS rf SQUID operation, Physica C 372–376 (2002) 282–286.